



Available online at [www.sciencedirect.com](http://www.sciencedirect.com)

**ScienceDirect**

journal homepage: [www.elsevier.com/locate/bbe](http://www.elsevier.com/locate/bbe)



## Original Research Article

# Automated segmentation and classification of brain stroke using expectation-maximization and random forest classifier



Asit Subudhi<sup>a</sup>, Manasa Dash<sup>b</sup>, Sukanta Sabut<sup>c,\*</sup>

<sup>a</sup>Department of ECE, ITER, SOA Deemed to be University, Odisha, India

<sup>b</sup>Department of Mathematics, Silicon Institute of Technology, Bhubaneswar, Odisha, India

<sup>c</sup>School of Electronics Engineering, KIIT Deemed to be University, Odisha, India

## ARTICLE INFO

### Article history:

Received 11 January 2019

Received in revised form

22 April 2019

Accepted 23 April 2019

Available online

### Keywords:

Brain stroke

MRI

Expectation-maximization

OCSF scheme

Classifier

## ABSTRACT

Magnetic resonance imaging (MRI) is effectively used for accurate diagnosis of acute ischemic stroke. This paper presents an automated method based on computer aided decision system to detect the ischemic stroke using diffusion-weighted image (DWI) sequence of MR images. The system consists of segmentation and classification of brain stroke into three types according to The Oxfordshire Community Stroke Project (OCSF) scheme. The stroke is mainly classified into partial anterior circulation syndrome (PACS), lacunar syndrome (LACS) and total anterior circulation stroke (TACS). The affected part of the brain due to stroke was segmented using expectation-maximization (EM) algorithm and the segmented region was then processed further with fractional-order Darwinian particle swarm optimization (FODPSO) technique in order to improve the detection accuracy. A total of 192 scan of MRI were considered for the evaluation. Different morphological and statistical features were extracted from the segmented lesions to form a feature set which was then classified with support vector machine (SVM) and random forest (RF) classifiers. The proposed system efficiently detected the stroke lesions with an accuracy of 93.4% using RF classifier, which was better than the results of the SVM classifier. Hence the proposed method can be used in decision-making process in the treatment of ischemic stroke.

© 2019 Published by Elsevier B.V. on behalf of Nalecz Institute of Biocybernetics and Biomedical Engineering of the Polish Academy of Sciences.

## 1. Introduction

In stroke, some part of the brain cells dies due to lack of oxygen/nutrients by blockage of an artery to the brain. Worldwide, stroke is third cause of death and main cause

of disability. It commonly occurs in low- and middle-income counts [1]. Efforts are required to improve the diagnosis process for effective use of therapeutic applications. It is necessary to identify the damage part of the brain using MRI, therefore computer based diagnosis process can be used effectively for predicting the occurrence of the disease [2]. Use

\* Corresponding author at: School of Electronics Engineering, KIIT Deemed to be University, Bhubaneswar, Odisha 751031, India.

E-mail address: [sukanta.sabatfet@kiit.ac.in](mailto:sukanta.sabatfet@kiit.ac.in) (S. Sabut).

<https://doi.org/10.1016/j.bbe.2019.04.004>

0208-5216/© 2019 Published by Elsevier B.V. on behalf of Nalecz Institute of Biocybernetics and Biomedical Engineering of the Polish Academy of Sciences.

of machine learning approach has advantage in automated process for detecting the stroke lesion which is the main focus of the research in present days [3]. The affected part in the brain can be detected accurately using DWI modality which is sensitive to change in water diffusion that happens in acute stroke. Therefore DWI modality images are more suitable for early detection of stroke lesions [4,5]. The objects from an image can be segmented by using different algorithms based on the thresholding and clustering approach [6–8]. The affected part of the brain is segmented efficiently using Fuzzy C-Mean (FCM) clustering methods. Zotin et al. [9] presented an automated process to segment the brain lesion using DWI modality of MR images based on Fuzzy C-Means. The method precisely segmented the lesions and achieved good results with Jacquard index of 0.547 and Dice indices of 0.687. In an automated work, Seghier et al. [2] identified the lesion by adopting fuzzy clustering using T1-weighted (T1w) MRI datasets. The adaptive FCM algorithm also found to be effective in lesion detection in brain MR data [8]. Maier et al. [10] presented a new approach for automatic segmentation of sub-acute ischemic stroke using brain T1-weighted MRI. The features were extracted based on their intensity and classified with extra tree forest classifier. The method achieved higher segmentation accuracy with a Dice coefficient of 0.65. A fuzzy segmentation method was presented which used the low similarity of intensity for finding regions of lesions using a single MRI based segmentation [11]. A computer-assisted method was presented by Tsai et al. [12] based on empirical threshold and atlas information for segmentation of cerebral infarcts by using T1-weighted, and DWI modality. In this approach achieved an average sensitivity of 84.154% and specificity of 99.9% in detecting cerebral infarcts.

In segmentation process, the EM algorithm partially assigns data points to different clusters based on highest probability associates value [13]. The expectation-maximization (EM) based on Gaussian mixture model (GMM) is commonly used for object segmentation in brain MRI images [14]. The maximum likelihood function of EM algorithm estimates the optimized parameters using probabilistic models. In EM algorithm, the highest probability associates value is assigned into different clusters in the segmentation process [15]. In the presence of multiple local maxima, it does not guarantee convergence to the global maxima [16]. Niu et al. [17] presented a report on the use of random swap EM (RSEM) algorithm for color image segmentation. Huang and Liu presented an unsupervised method based on the EM algorithm to find the approximate parameters of the Gaussian mixtures model (GMM) to classify the image [18]. The result with split and merge approaches was compared with the characteristics of the variants. It was found that RSEM performed better than the other methods. Mahjoub and Kalti introduced image segmentation based on Bayesian algorithm using finite mixtures model [19]. An EM algorithm is used to estimate parameters of the GMM to provide clusters in the field of pattern recognition. They achieved significant improvement compared to the standard version of EM algorithm.

Marroquin et al. [20] presented an efficient and automated method for 3D segmentation of brain MR scans based on the EM algorithm for a speedy and accurate optimal segmentations of the brain from the non-brain tissue. Tian et al. [21]

proposed a hybrid model based on genetic and variational EM (GA-VEM) algorithm for segmentation of brain MR images. The variational EM algorithm is used to estimate the GMM and the genetic algorithm is used to initialize the hyper-parameters in order to achieve global optimization. The hybrid algorithm overcomes the drawbacks of traditional EM based methods and improved the segmentation performance. In another hybrid approach, the Fuzzy C-Means and EM algorithms are combined and used successfully to segment the MR brain images. The intensity non-uniformity and noise effect were overcome using EM and FCM with spatial information and bias correction [22]. Recently, Kwon et al. [23] used the clustering approach based on watershed transformation and EM algorithm for effective segmentation of MR brain images. Rouainia et al. [24] successfully detected the lesions in brain MRIs using EM algorithm by building a statistical model from the data itself. However we did not find any article which uses the EM algorithm for stroke lesion segmentation, therefore in this paper we proposed an automated method to detect stroke lesion based on EM approach that forms the clusters having same intensity of pixels which is separated by selecting a threshold generated by binary mask. The EM based segmented region has been further enhanced by FODPSO approach to improve accuracy of detection. The method was validated in 192 brain images of DWI sequences collected from stroke patients. The important morphological and statistical features were extracted from the segmented images and the features set was then classified with SVM and RF classifier to distinguish three types of stroke.

## 2. Methodology

In this work, the stroke lesion was segmented by EM algorithm using brain MRIs. The block diagram of the proposed detection approach of stroke lesion is shown in Fig. 1. Types of stroke were classified according to The Oxford Community Stroke Project classification (OCSP) and are also known as the Bamford or Oxford classification [25]. In this classification scheme, the patients with cerebral infarction were allocated to one of three groups according to the presence of signs and symptoms. Depending on the initial symptoms and its extent of the symptoms, the stroke episode is classified as Total Anterior Circulation Stroke syndrome (TACS); Partial Anterior Circulation Stroke syndrome (PACS); Lacunar Stroke syndrome (LACS). All the used 192 different slices MRI datasets of DWI sequences are classified according to OCSP that includes PACS 122, LACS 36, and TACS 34 numbers. All brain images were acquired with a Signa HDxT 1.5T Optima Edition (GE Healthcare, Waukesha, WI), DWI sequence having slice thickness of 5 mm with a gap of 1 mm and an ADC map with  $b = 1000 \text{ s/mm}^2$  are considered for testing.

### 2.1. Expectation-maximization process

The expectation-maximization (EM) algorithm uses the probabilistic models to compute the maximum likelihood estimates of unknown parameters [13]. The algorithm is an iterative method, which solves the maximization problem. The maximum-likelihood model is used to find the “best fit”

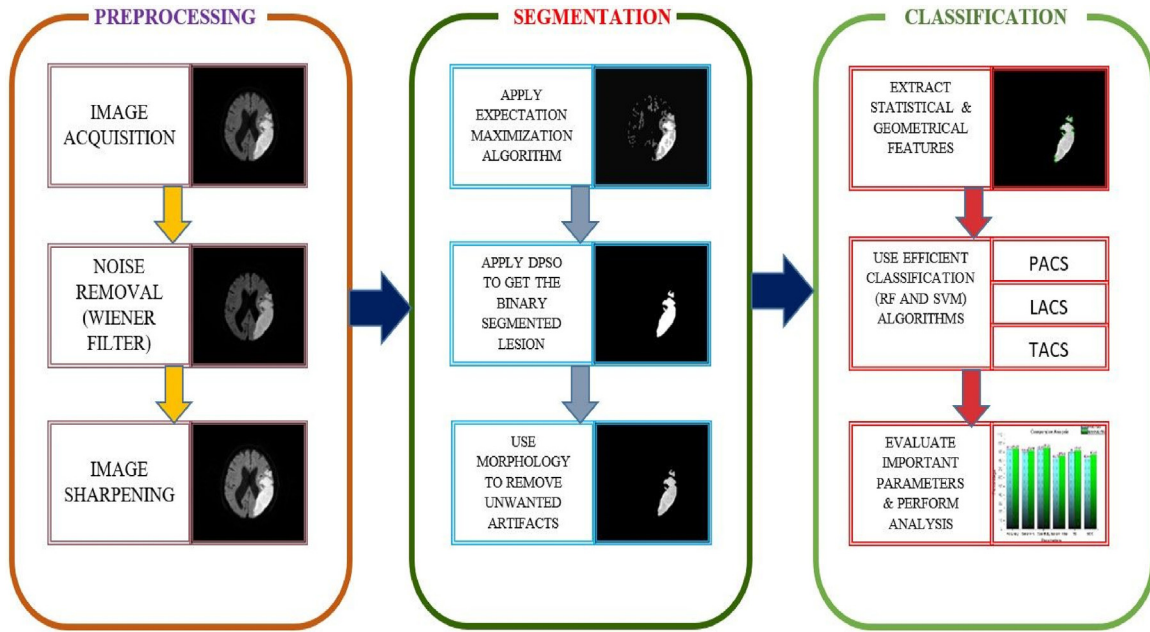


Fig. 1 – Block diagram of the proposed EM based method for lesion detection.

for a data set by choosing random values. The best fit is estimated in an unsupervised manner by an iterative process using the EM algorithm in an incomplete/missing data points [26,27]. The “best fit” is calculated by maximum likelihood estimation for a set of complete data with  $\theta = \xi$  as shown in Fig. 2. For a missing data set, the complex EM algorithm is efficient enough to catch the model parameters. The lost data points are selected randomly by the EM process and these data are used to predict the preceding set of data. The obtained fresh values are again used to create improved prediction of the initial set, and finally the algorithm converges to a fixed point for getting the best fit. The value of  $\theta$  can be maximized with the knowledge of  $w_i$ . The process starts with a prediction for  $\theta$ , then calculate  $z$ , then update  $\theta$  using this new value for  $z$ , and it repeats till convergence.

The EM algorithm can be generalized as an estimation problem having a training set  $\{a^{(1)}, a^{(2)}, \dots, a^{(m)}\}$ , having  $m$  independent samples. These set of training parameters are required to fit with a model  $P(x, z)$ , where the corresponding likelihood is expressed as

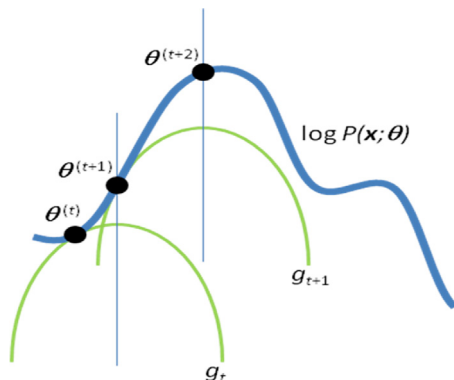


Fig. 2 – The convergence of EM algorithm [23].

$$j(\xi) = \sum_{i=1}^m \log p(x, \xi) \quad (1)$$

The maximum likelihood estimation of  $\xi$  is quite difficult where the easy estimation is feasible if we can observe the latent variable  $z^{(1)}$ . The EM algorithm can then be described as a combination of two stages where in the first stage we construct a lower bound on  $j$  called as E step. Further we optimize the lower bound, which is referred as M step.

The EM algorithm has been used effectively for missing values in a data set to find a likelihood function. The density of the samples is expressed as

$$p(x|\xi) = \prod_{i=1}^N p(x_i|\xi) = \mathcal{L}(\xi|x) \quad (2)$$

with  $x$  representing the sample data of size  $N$ , the function  $\mathcal{L}(\xi|x)$  is called the likelihood function. The objective of the process is to estimate  $\xi$  that optimize the maximal value of  $\mathcal{L}$ .

Assume that for a complete data set  $z = (x, y)$  and the association between the missing and detected values is represented by a joint density function given by

$$p(z|\xi) = p(x, y|\xi) = p(x|x, \xi)p(x|\xi) \quad (3)$$

We can define a new likelihood function with this new density function,

$$\mathcal{L}(\xi|z) = \mathcal{L}(\xi|x, y) = p(x, y|\xi) \quad (4)$$

Initially, the algorithm finds the estimated value for the entire-data set with log-likelihood of  $\log p(x, y|\xi)$  with respect to the unidentified data, detected data  $x$ , and the existing

estimated parameter. The estimation of current parameter is expressed as

$$Q(\xi, \xi^{(i-1)}) = E\{\log_p(x, y|\xi)|x, \xi^{(i-1)}\} \quad (5)$$

where  $\xi^{(i-1)}$  are the current estimated parameters used to calculate the expectation value and  $\xi$  are the latest parameters that is optimize to increase  $Q$  value.

To maximize the expectation, we need to find

$$\xi^{(i)} = \underset{\xi}{\operatorname{argmax}} Q(\xi, \xi^{(i-1)}) \quad (6)$$

In this work, the image was segmented with EM algorithm in a periodic means to converge with the result. The input image is distributed into different groups with probability of similar intensity of the pixels from normal and affected tissues. By the iteration process, the center point of the cluster is reformed, until to attain a center of a fixed cluster. The details of EM process is defined in the following equations [24]:

- Initialize  $m_i$ ,  $\sigma_i$  and  $c_i$  as the mean, co-variance and mixing co-efficient respectively to calculate

$$\log I(\xi) = \sum_{k=1}^N \log \left[ \sum_{i=1}^M c_i P(x_k | m_i, \sigma_i) \right] \quad (7)$$

where  $I(\xi)$  is described as the associated log-likelihood function.

- Further we can approximate the expectation as

$$T_{kl} = \frac{c_l P(x_k | m_l, \sigma_l)}{\sum_{t=1}^M c_t P(x_k | m_t, \sigma_t)}, \quad 1 \leq l \leq M, 1 \leq t \leq N \quad (8)$$

- Perform maximization as

$$m_l^{new} = \frac{1}{N_l} \sum_{k=1}^N T_{kl} x_k, \quad 1 \leq l \leq M \quad (9)$$

- The updated co-variance is given as

$$\sigma_l^{new} = \frac{1}{N_l} \sum_{k=1}^N T_{kl} (x_k - m_l^{new})(x_k - m_l^{new})^t, \quad 1 \leq l \leq M$$

where  $x$  is the characteristic vector,  $k$  represents the probability density function.

The structure of the mixture model is given by

$$P(x|\xi) = \sum_{i=1}^M c_i P(x|m_i, \sigma_i) \quad (10)$$

## 2.2. Fractional-order Darwinian PSO (FODPSO)

The FODPSO is an advanced optimization method of Darwinian PSO, which is having an advantage of controlling the convergence rate of the process [28]. The numerical methods keep properties of fractional differential equations (FDEs), with  $\alpha$  is an extension of ordinary differential equations with Euler scheme. The signal  $x(t)$  the discrete time system is elaborated with the concept of the fractional differential with  $\alpha \in \mathbb{C}$  and described as

$$D^\alpha[x(t)] = \frac{1}{T^2} \sum_{k=0}^r \frac{(-1)^k \Gamma(\alpha+1) x(t-kT)}{\Gamma(k+1) \Gamma(\alpha-k+1)} \quad (11)$$

where  $\Gamma$  is the gamma function,  $T$  is the sampling period and  $r$  is the truncation order.

The proposed method of FODPSO is having an advantage that while we obtain a finite series upon applying derivative to an integer-order, whereas the fractional-order derivative implies an infinite number of terms. We consider the local operators are integer derivatives and memories of all past events are fractional derivatives. The effect of past events reduces with respect to time.

Considering  $w = 1$  for a specific swarm

$$v_n^s[t+1] = v_n^s[t] + \sum_{i=1}^2 \rho_i r_i (x_{in}^s[t] - x_n^s[t]) \quad (12)$$

Assuming  $T = 1$  and based on Grunwald–Letnikov fractional derivative, we have

$$D^\alpha[v_n^s[t+1]] = \sum_{i=1}^2 \rho_i r_i (x_{in}^s[t] - x_n^s[t]) \quad (13)$$

Using fractional calculus the order of velocity derivative is generalized with  $1 < \alpha < 1$  that leads to smooth variation and enhanced memory. If we remove the concept of memory from FODPSO, i.e., with  $\alpha = 1$ , then the process leads to DPSO. Considering the Grunwald–Letnikov fractional difference of the order of the generic discrete signal  $x(t)$  is described as

$$v_n^s[t+1] = - \sum_{k=1}^r \frac{(-1)^k \Gamma(\alpha+1) v_n^s(t+1-kT)}{\Gamma(k+1) \Gamma(\alpha-k+1)} + \sum_{i=1}^2 \rho_i r_i (x_{in}^s[t] - x_n^s[t]) \quad (14)$$

In FODPSO particles strive to find the best solution for their own “survival”, with the perk of intrinsically having a memory of past decisions which avoids the problem of convergence in traditional optimization processes.

## 2.3. Texture features based on the GLCM algorithm

Extraction of important features which identifies the characteristics of an object is a task to improve the classification accuracy [29]. Haralick et al. [30] proposed the use of the Gray Level Co-occurrence Matrix (GLCM) approach for extracting features that consists of morphological and statistical information. The feature set consists of textural feature and statistical values to identify regions of interest. In this work, we have used mean, standard deviation, contrast, entropy, correlation, energy, inverse difference moment, variance and sum average.

## 2.4. Classifiers

### 2.4.1. Random forest (RF) classifier

The RF algorithm is widely used for classification of diseases in medical image analysis [31]. It was found to be effective in classifying the brain stroke images [29]. The disadvantages of overfitting of decision tree algorithm are reduced in RF

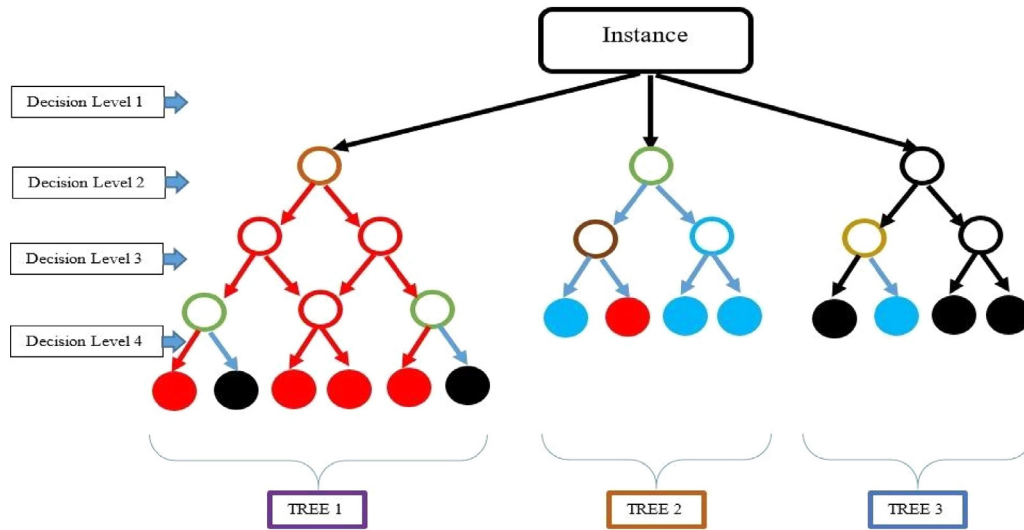


Fig. 3 – The functional diagram of random forest classifier.

by combining multiple decision trees to obtain the accurate final decision.

**Decision trees:** A decision tree is a predictive model represented by graphically and used effectively to classify the data set. The model determines the best decisions in the analysis process by splitting the data set into smaller subsets. During the learning phase, the model maximizes the information gain  $I$  in a given node which is represented by

$$I = H(S) - \sum_{i \in L, R} \frac{|S^i|}{|S|} H(S^i) \quad (15)$$

where  $H$  is the entropy, input data is  $S$  that is splitted into two subset nodes  $S^L$  and  $S^R$ .

**Random forest classifier:** The RF classifier is a supervised method in which the multiple decision trees are used to create a forest as shown in Fig. 3. The RF algorithm works better when the large dataset. The forest is more robust when higher

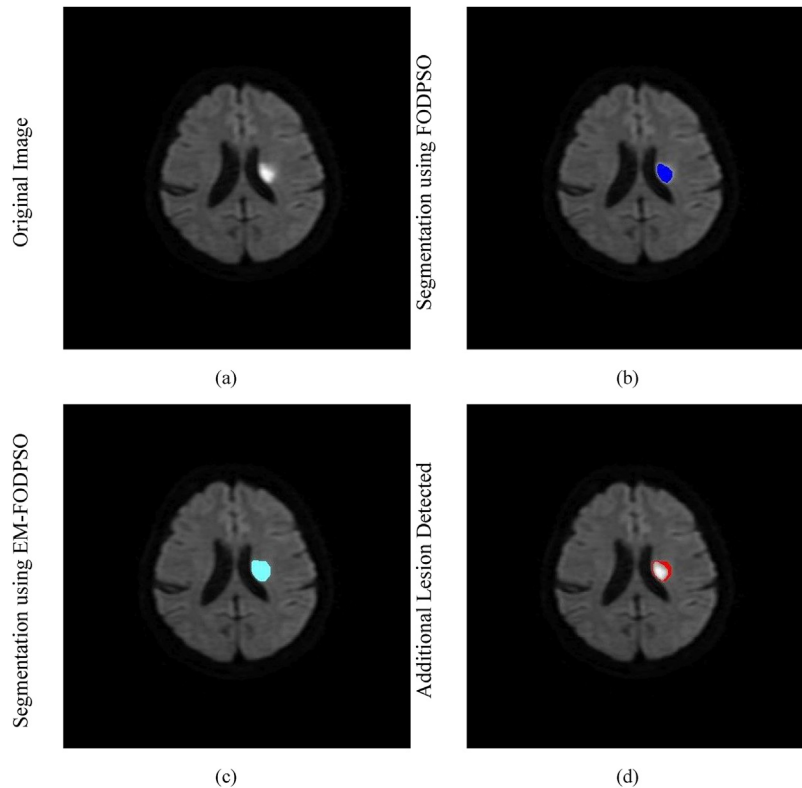


Fig. 4 – Example of segmentation output on a small lesion: (a) original image; (b) segmented lesion using FODPSO in blue color; (c) segmented lesion using EM-FODPSO in cyan color; (d) additional lesion detected using EM-FODPSO in red color.



number of trees is used in decision making process [32]. Generally a leaf is considered for expansion in each step of the construction of tree. The dataset is randomly divided into two parts with similar structure.

The margin function of the algorithm is expressed as

$$mg(X, Y) - \alpha v_k I(h_k(X) = Y) - \max_{j \neq Y} \alpha v_k I(h_k(X) = j) \quad (16)$$

where  $I(\cdot)$  is the indicator function,  $h_1(x), h_2(x), \dots, h_k(x)$  are the ensemble of classifiers and  $Y, X$  are random vector.

The error is given by

$$PE^* = P_{X,Y}(mg(X, Y) < 0) \quad (17)$$

In RF,  $h_k(X) = h(X, \Theta_k)$

The margin function for an RF is given by the equation

$$mr(X, Y) = P_{\Theta}(h(X, \Theta) = Y) - \max_{j \neq Y} P_{\Theta}(h(X, \Theta) = j) \quad (18)$$

and the strength of the classifier  $\{h(x, \Theta)\}$  is given by

$$s = E_{X,Y} mr(X, Y) \quad (19)$$

The RF algorithm is an efficient model that builds the multiple decision trees and merges them into a single tree

to having highest prediction accuracy. The RF algorithm is described in the following steps:

Step 1: To start with a given data set  $D_1$  having  $m \times n$  matrix, a new dataset  $D_2$  is created from the original data by sampling and removing one-third of the row data.

Step 2: The model is trained to generate the new dataset from the reduced samples and estimates the unbiased error.

Step 3: At each node point in the data set,  $n_1$  column is selected from total  $n$  columns.

Step 4: In this algorithm, several trees grow simultaneously and the final prediction is done with the collection of individual decisions to obtain the best classification accuracy.

#### 2.4.2. Support vector machine classifier

The SVM is a commonly used machine learning approach of classification, which classifies the information with better accuracy and with minimization principle from unseen patterns [33]. It analyses a large amount of data and classify them into different classes having identity data patterns. A hyperplane is used in partitioning process and makes a margin between the classes that represents the longest distance between closest data points. We classify the input data by selecting an appropriate hyperplane. It can be defined the support vector as the co-ordinate of individual observation or feature.

The SVM uses a set of a training dataset  $D$  which can be mathematically expressed as

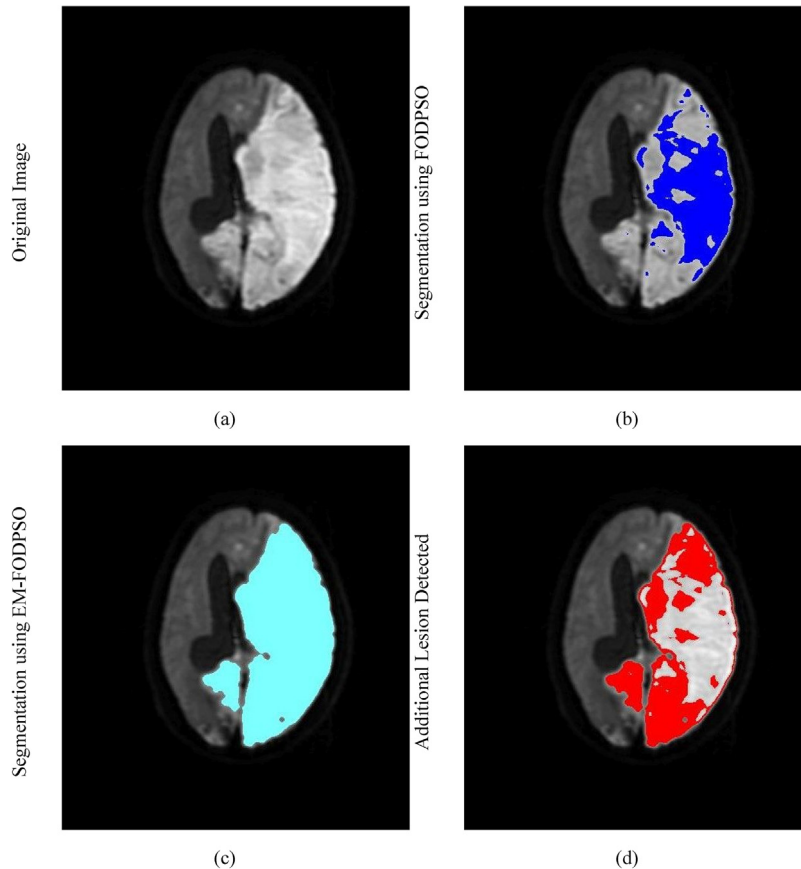


**Fig. 5 – Example of segmentation output on a large lesion: (a) original image; (b) segmented lesion using FODPSO in blue color; (c) segmented lesion using EM-FODPSO in cyan color; (d) additional lesion detected using EM-FODPSO in red color.**

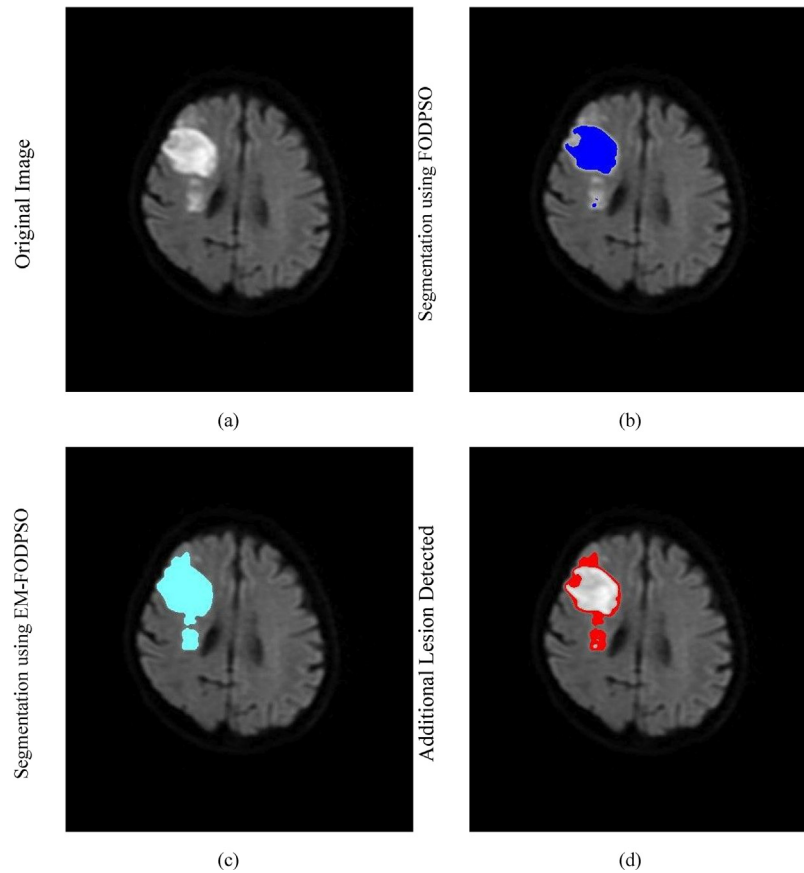


**Fig. 6 – Example of segmentation process in a slice having multiple lesions: (a) original image; (b) segmented lesion using FODPSO in blue color; (c) segmented lesion using EM-FODPSO in cyan color; (d) additional lesion detected using EM-FODPSO in red color.**

$$D = \{(x_1y_1), (x_2y_2), \dots, (x_Ny_N)\} \quad (20)$$

where  $x_i$  is an  $n$ -dimensional real vector and  $y_i$  is either  $-1$  or  $+1$  indicating the class to which  $x$  belongs.

We can express the SVM classification function as

$$F(x) = w \cdot x - b \quad (21)$$

where  $w$  is the weight vector and  $b$  is the bias.

The classification function is expressed as

$$y_i(w \cdot x_i - b) > 0, \forall (x_i, y_i) \in D \quad (22)$$

The points on  $D$  if correctly classified with the above equation then it is called as linearly separable system.

The hyperplane is used to maximize the margin which is the distance from the hyperplane to the closest data point and is written by

$$\text{margin} = \frac{1}{\|w\|} \quad (23)$$

Maximizing the margin becomes minimizing  $\|w\|$ . Thus SVM can be observed as an optimization problem to

$$\text{minimize : } Q(w) = \frac{1}{2} \|w\|^2 \quad (24)$$

$$\text{subject to : } y_i(w \cdot x_i - b) \geq 1, \forall (x_i, y_i) \in D$$

**Table 1 – The areas of segmented lesion for both the methods in randomly selected images.**

Image No.	FODPSO		EM-FODPSO	
	Area (pixels)	Avg. intensity	Area (pixels)	Avg. intensity
32	12,931	210.84	26,834	188.09
62	2863	210.98	4748	184.57
20	399	197.25	632	169.65

**Table 2 – The confusion matrix and different measures of the classification.**

3 fold		PREDICTED				Measures				
		PACS	LACS	TACS		TP	TN	FP	FN	
TRUE	PACS	32	1	0	33	32	30	1	1	PACS
	LACS	0	17	2	19	17	44	1	2	LACS
	TACS	1	0	11	12	11	50	2	1	TACS
		33	18	13	64					

**Table 3 – The evaluated results of different parameters for 3-class of stroke.**

	Acc	Sensitivity	Specificity	Jaccard	Dice
PACS	0.96875	0.96969697	0.96774194	0.941176	0.969697
LACS	0.953125	0.89473684	0.97777778	0.85	0.918919
TACS	0.953125	0.91666667	0.96153846	0.785714	0.88
Weighted average	0.961182	0.9375	0.969558	0.884959	0.937804

**Table 4 – The results of FODPSO method obtained in SVM classifier.**

Fold no.	Sensitivity	Specificity	Accuracy	Jaccard index	DSI
2	0.93	0.94	0.95	0.87	0.93
3	0.89	0.94	0.93	0.81	0.89
4	0.88	0.93	0.91	0.78	0.88
5	0.92	0.95	0.95	0.86	0.92
6	0.91	0.93	0.93	0.83	0.91
7	0.85	0.95	0.91	0.76	0.86
8	0.88	0.91	0.91	0.78	0.88
9	0.85	0.87	0.88	0.74	0.85
10	0.84	0.92	0.89	0.74	0.84
Avg.	0.883	0.926	0.917	0.796	0.884

**Table 5 – The results of EM-FODPSO method obtained in SVM classifier.**

Fold no.	Sensitivity	Specificity	Accuracy	Jaccard index	DSI
2	0.95	0.96	0.96	0.90	0.95
3	0.91	0.95	0.93	0.83	0.91
4	0.92	0.95	0.94	0.85	0.92
5	0.95	0.96	0.96	0.90	0.95
6	0.91	0.95	0.93	0.83	0.91
7	0.89	0.94	0.93	0.80	0.89
8	0.92	0.95	0.94	0.85	0.92
9	0.80	0.89	0.87	0.68	0.80
10	0.89	0.97	0.93	0.82	0.90
Avg.	0.904	0.946	0.932	0.828	0.905

Assume the training data have  $N$  pairs  $(x_1y_1), (x_2y_2), \dots, (x_Ny_N)$  with  $x_i \in \mathbb{R}^p$  and  $y_i \in \{-1, 1\}$ .

Let a hyperplane be  $\{x : f(x) = x^T\beta + \beta_0 = 0\}$ , where  $\beta$  is a unit vector,

$$G(x) = \text{sign}[x^T\beta + \beta_0]C \quad (25)$$

The function  $f(x)$  resulted from signed distance from a point  $x$ .

### 3. Experimental results

The stroke lesion was segmented using EM based algorithm in all the 192 brain MR images taken for evaluation. The

features set was obtained from the segmented regions and classified with SVM, RF classifiers. The binary mask was used to separate the healthy and affected tissue to form separate clusters in order to obtain the feature set. The structure of the lesion was reconstructed by the morphological operations like erosion and dilation. The output images of EM method were then further enhanced by FODPSO algorithm to achieve better accuracy results. The effectiveness of the method was evaluated with different parameters, i.e., sensitivity (Se), specificity (Sp), accuracy (Acc), dice similarity index (DSI), and Jaccard index (JI), from the confusion matrix [34].

An example of original stroke affected image is shown in Fig. 4, which is de-noised with a median filter, a binary mask is generated by applying a threshold and finally the structure



of the lesion is segmented with the morphological approach (marked with color boundary). The segmented output using EM-FODPSO method into three types of lesions randomly selected from the collected images is shown in Figs. 4–6. From the visual observation of the binary mask generated by the automated method confirmed that the boundary of the stroke-induced lesion was retrieved accurately in almost all the slices. It is also observed that the proposed EM-FODPSO based method was able to detect additional areas that are not detected by the FODPSO method alone, as shown in red color in the segmented images. These additional areas are generally categorized by reduced image intensity that is fully or partially affected by stroke in different types of lesion sizes and shapes. Table 1 shows the value of pixels used to measure the areas of the detected lesion. It has been observed that EM-FODPSO based approach has large pixel size with lower intensities. Tables 2 and 3 are shown as an example of confusion matrix and classification into three types of stroke.

Finally, we have evaluated the efficiency of the method to detect lesion structure on a large dataset. Thirty-five different features were extracted to form a feature set and then classified using SVM and RF classifiers in order to identify the stroke types. The feature matrix is then used to train the classifier in the 10-fold cross-validation process. The validation results are illustrated in Tables 4–7 using both the classifiers. The better segmentation result is indicated with the higher index value. The proposed approach achieved an average accuracy of 0.94 in RF classifier which was better than the results obtained in SVM classifier having accuracy of 0.92. Also the values of all evaluated parameter was better in RF classifier

as observed from the tables. The performance measures of FODPSO and EM-FODPSO methods are plotted in Figs. 7–12 for comparative analysis. Finally, all measured parameters are presented in Fig. 13 for an effective comparison of results in SVM and RF classifiers.

#### 4. Discussion

The normal and affected tissue in the brain region can be separated effectively by using EM based process. It is based on clustering approach that allots the similar intensity value to a particular cluster in order to separate two regions. The evaluated measures JI and DSI indicate the quality of the image segmentation done for the separation of affected lesions. The comparison results with other published articles are presented in Table 8. An automated method based on the detection outlier voxels has been reported for lesion identification from a single image of brain MRI [2]. The model combines the process to segment the gray and white matter in normalized images, and adopted a fuzzy clustering approach for identification of outlier voxels in normalized. The lesion boundaries were traced precisely with dice similarity of 0.64. Muda et al. [35] presented a fully automated algorithm called ATLAS which is a standard method that helps in decision-making process to manage acute stroke patients. The ATLAS based algorithm management able to delineate the core lesion of stroke with dice co-efficient of 0.61 in DWI modality of MRI. Griffs et al. [36] developed an automated segmentation approach based on Naive Bayes classifier to detect stroke

**Table 6 – The results of FODPSO method obtained in RF classifier.**

Fold no.	Sensitivity	Specificity	Accuracy	Jaccard index	DSI
2	0.94	0.96	0.96	0.89	0.94
3	0.91	0.95	0.93	0.83	0.91
4	0.92	0.94	0.94	0.85	0.92
5	0.92	0.95	0.95	0.86	0.92
6	0.84	0.90	0.89	0.73	0.84
7	0.85	0.90	0.90	0.74	0.85
8	0.92	0.95	0.94	0.85	0.92
9	0.86	0.92	0.89	0.75	0.86
10	0.89	0.97	0.92	0.81	0.89
Avg.	0.894	0.937	0.924	0.812	0.894

**Table 7 – The results of EM-FODPSO method obtained in RF classifier.**

Fold No.	Sensitivity	Specificity	Accuracy	Jaccard index	DSI
2	0.95	0.94	0.96	0.90	0.94
3	0.94	0.97	0.93	0.88	0.94
4	0.93	0.95	0.95	0.84	0.92
5	0.91	0.95	0.92	0.84	0.93
6	0.90	0.95	0.93	0.85	0.91
7	0.94	0.94	0.90	0.75	0.89
8	0.92	0.98	0.95	0.86	0.92
9	0.95	0.98	0.93	0.91	0.95
10	0.89	0.97	0.94	0.82	0.90
Avg.	0.925	0.958	0.934	0.85	0.922

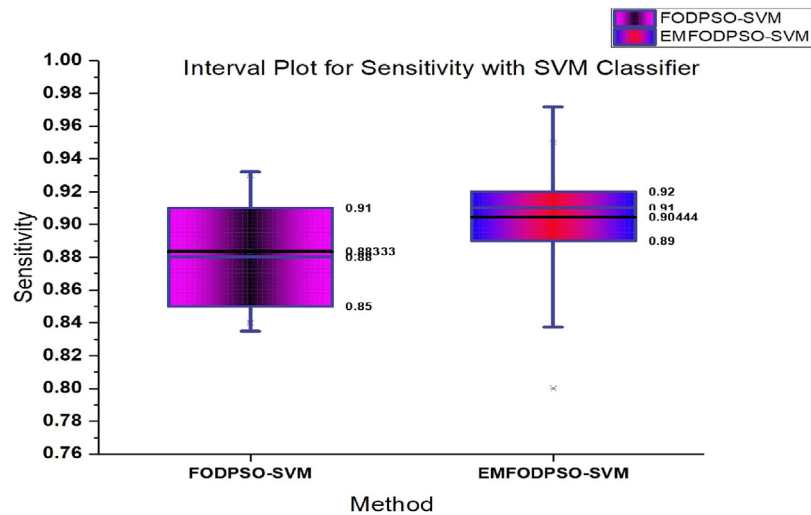


Fig. 7 – Plots of sensitivity versus different folds obtained for two methods using SVM classifier.

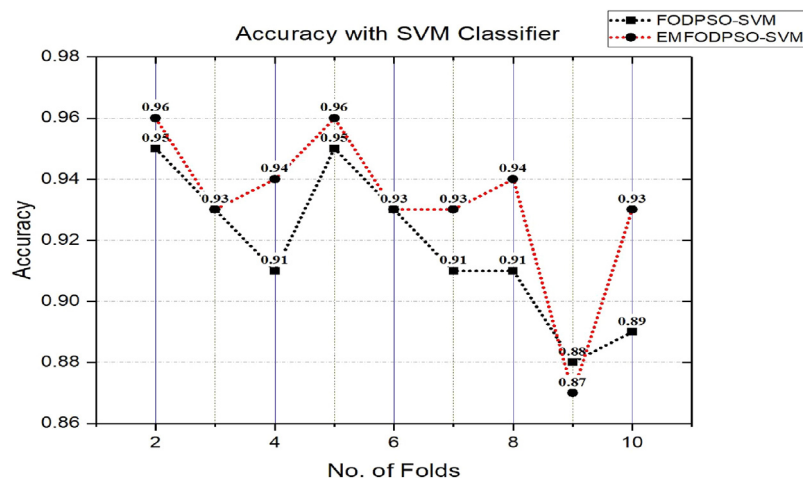


Fig. 8 – Plots of accuracy versus different folds obtained for two methods using SVM classifier.

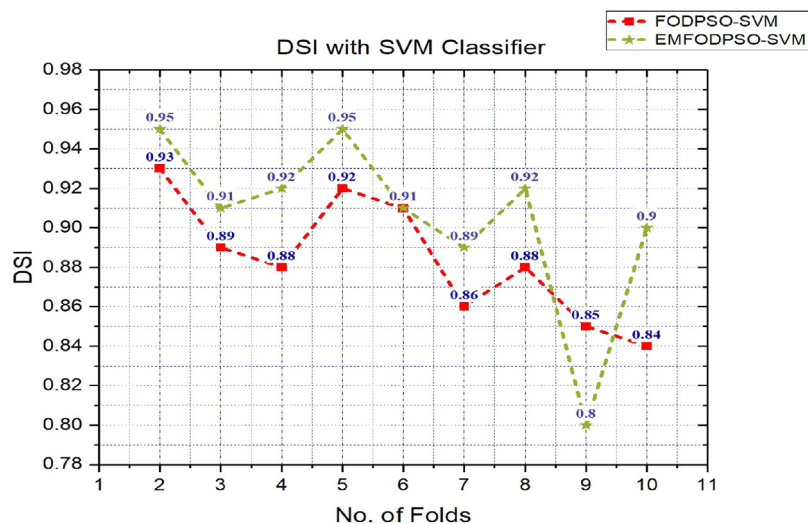


Fig. 9 – Plots of DSI versus different folds obtained for two methods using SVM classifier.

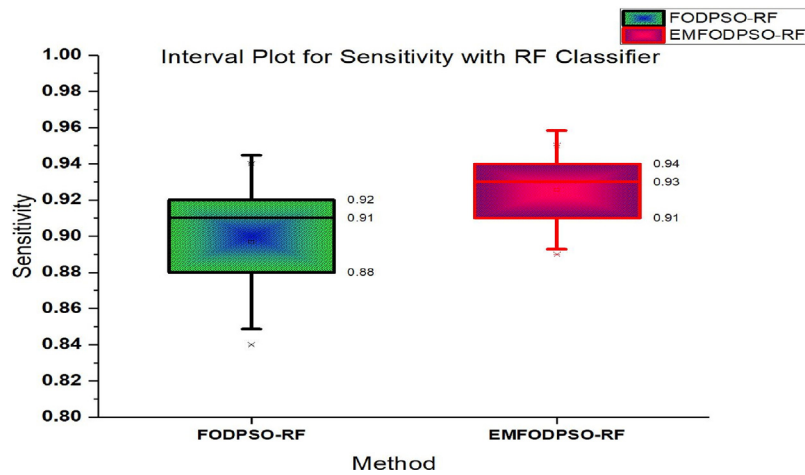


Fig. 10 – Plot of sensitivity obtained in RF classifier using 10-fold validation process.

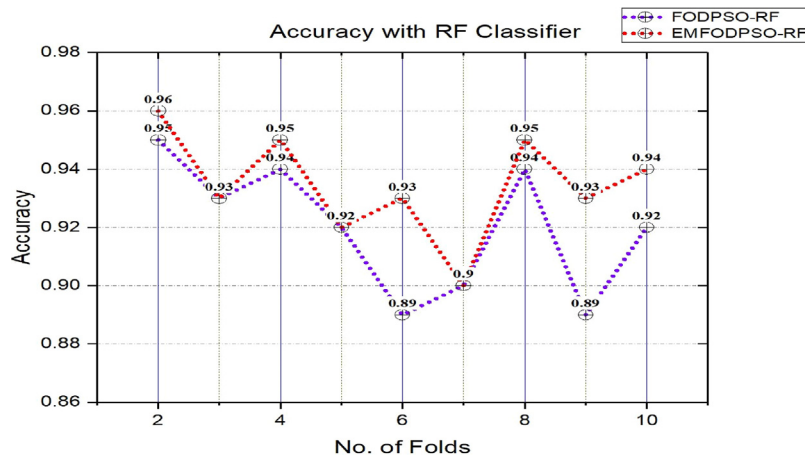


Fig. 11 – Plots of accuracy versus different folds obtained for two methods using RF classifier.

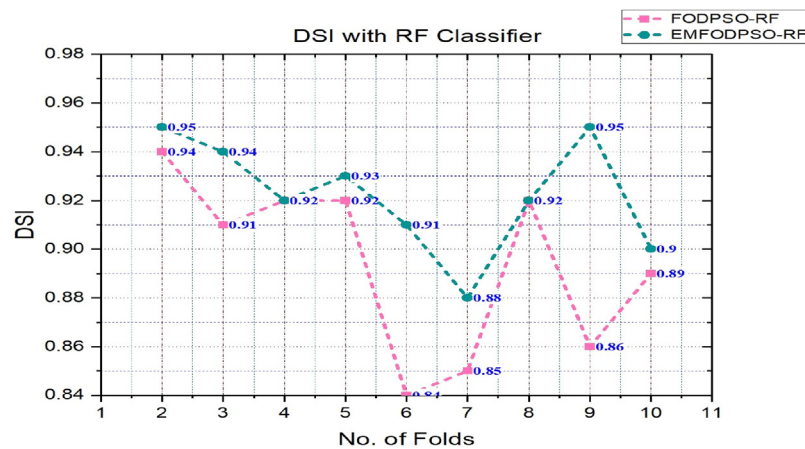


Fig. 12 – Plots of DSI versus different folds for two methods obtained using RF classifier.

lesions with dice similarity index of 0.66. In 2014, Mitra et al. [37] presented a Bayesian–Markov Random Field (MRF) model to segment and classify the chronic stroke lesion using FLAIR modality of MRI. They achieved a mean dice similarity

coefficient of 0.60 using RF classifier. Different examples of affected images with small, large and multiple lesions of the proposed method are presented. The method achieved good classification results with a sensitivity of 0.92, an accuracy of

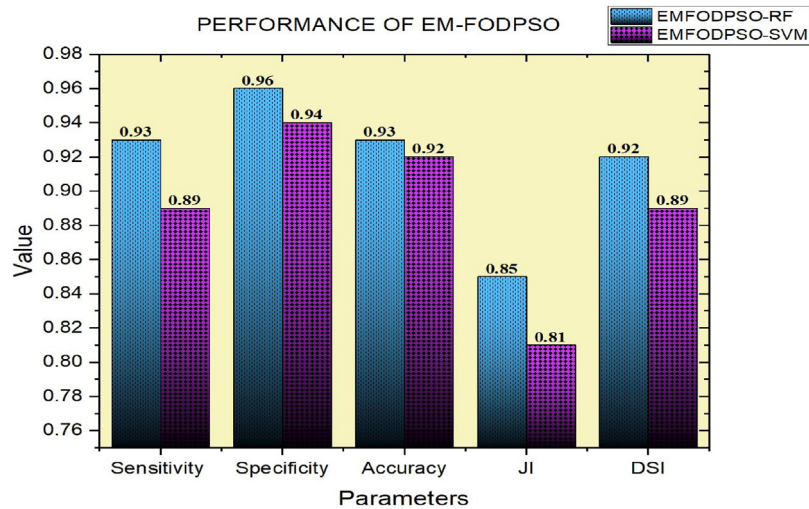


Fig. 13 – Comparison of results obtained by SVM and RF classifiers.

Table 8 – The comparison of obtained results with few published articles.

Authors	Methods	Classifier	DSI
Seghier et al. [2]	Generative model	Fuzzy clustering	0.64
Tsai et al. [12]	FCM clustering	Unsupervised classification	0.89
Maier et al. [10]	Intensity derived image features	Extra tree forest framework	0.65
Maier et al. [40]	Fuzzy clustering approach	Random Decision Forest	0.72
Muda et al. [35]	Fuzzy C-Means (FCM) algorithm	Expert system	0.61
Griffs et al. [36]	Probabilistic tissue segmentation	Naive Bayes classifier	0.66
Mitra et al. [37]	Bayesian–Markov Random Field (MRF)	Random forest	0.60
Proposed method	EM-FODPSO	Random forest	0.93

0.94 and DSI of 0.92 using RF classifier, which is little better than the results of EM and fuzzy clustering approaches alone. Therefore we can say that EM-FODPSO based approach has the ability to detect lesion structure effectively. Our EM based approach has produced better results in comparison to other published work as shown in Table 6. In recent approach, artificial intelligence model effectively applied in medical signal and image analysis in object identification and classification directly from images by eliminating the step to extract the features, thus speed-up the process of classification [38,39]. Therefore deep neural network can be applied for effective analysis of ischemic stroke.

## 5. Conclusion

In this paper we have proposed an automated method to detect chronic brain stroke based on expectation-maximization clustering approach. The affected part of the brain was segmented by the EM algorithm and from the segmented part the features were extracted to make a set of features. The dataset is then classified into three types of stroke using random forest classifier. The affected lesion was clustered based on intensity similarity of the pixels which was identified with binary values. The lesion was segmented effectively with dice similarity index of 0.94 in the extracted features from the real-time images. The value of obtained results was better

compared to some of the published results, so the EM-FODPSO based segmentation method can be an alternate way to detect different sizes of stroke lesion using brain images. In future, we explore the possibility of determining the 3D volumetric value of the lesions.

## REFERENCES

- [1] Bonita R. Epidemiology of stroke. *Lancet* 1992;339:342–4.
- [2] Seghier ML, Ramackhansingh A, Crinion J, Leff AP, Price CJ. Lesion identification using unified segmentation-normalization models and fuzzy clustering. *Neuroimage* 2008;41:1253–66.
- [3] Wilke M, de Haan B, Juenger H, Karnath HO. Manual, semi-automated, and automated delineation of chronic brain lesions: a comparison of methods. *Neuroimage* 2011;56:2038–46.
- [4] Sezgin M, Sankur B. Survey over image thresholding techniques and quantitative performance evaluation. *J Electron Imaging* 2004;13:146–68.
- [5] Lutsep HL, Albers GW, DeCrespigny A, Kamat GN, Marks MP, Moseley ME. Clinical utility of diffusion-weighted magnetic resonance imaging in the assessment of ischemic stroke. *Ann Neurol* 1997;41:574–80.
- [6] Alpert S, Galun M, Brandt A, Basri R. Image segmentation by probabilistic bottom-up aggregation and cue integration. *IEEE Trans Pattern Anal Mach Intell* 2012;34:315–27.

- [7] Carson C, Belongie S, Greenspan H, Malik J. Blobworld: image segmentation using expectation-maximization and its application to image querying. *IEEE Trans Pattern Anal Mach Intell* 1999;24:1026–38.
- [8] Alipour S, Shanbehzadeh J. Fast automatic medical image segmentation based on spatial kernel fuzzy c-means on level set method. *Mach Vision Appl* 2014;25(6):1469–88.
- [9] Zotina A, Simonov K, Kurako M, Hamad Y, Kirillova S. Edge detection in MRI brain tumor images based on fuzzy C-means clustering. *Procedia Comput Sci* 2018;126:1261–70.
- [10] Maier O, Wilms M, von der Gablentz J, Kramer UM, Munte TF, Handels H. Extra tree forests for sub-acute ischemic stroke lesion segmentation in MR sequences. *J Neurosci Methods* 2015;240:89–100.
- [11] Pustina D, Coslett HB, Turkeltaub PE, Tustison N, Schwartz MF, Avants B. Automated segmentation of chronic stroke lesions using LINDA: lesion identification with neighborhood data analysis. *Hum Brain Mapp* 2016;37:1405–21.
- [12] Tsai JZ, Peng SJ, Chen YW, et al. Automatic detection and quantification of acute cerebral infarct by fuzzy clustering and histographic characterization on diffusion weighted MR imaging and apparent diffusion coefficient map. *BioMed Res Int* 2014;1–13.
- [13] Dempster AP, Laird NM, Rubin DB. Maximum likelihood from incomplete data via the EM algorithm. *J Royal Stat Soc* 1997;39(1):1–38.
- [14] Yoon UC, Kim JS, Kim IY, Kim SI. Adaptable fuzzy C-Means for improved classification as a preprocessing procedure of brain parcellation. *J Digit Imaging* 2001;14:238–40.
- [15] Lorenzo-Valdes M, Sanchez-Ortiz GI, Elkington AG, Mohiaddin RH, Rueckert D. Segmentation of 4D cardiac MR images using a probabilistic atlas and the EM algorithm. *Med Image Anal* 2004;8(3):255–65.
- [16] Sundberg R. An iterative method for solution of the likelihood equations for incomplete data from exponential families. *Commun Stat Simul Comput* 1976;5(1):55–64.
- [17] Niu M, Zhao Q, Li H. Comparison of EM-based algorithms and image segmentation evaluation. In: Huang DS, Jo KH, Wang L, editors. *Intelligent computing methodologies*. Lecture notes in Computer Science. 2014. p. 8589.
- [18] Huang ZK, Liu DH. Segmentation of color image using EM algorithm in HSV color space. *Proc Int Conf on Information Acquisition*; 2007.
- [19] Mahjoub MA, Kalti K. Image segmentation by adaptive distance based on EM algorithm. *Int J Adv Comp Sci Appl* 2011.
- [20] Marroquin JL, Vemuri BC, Botello S, Calderon E, Fernandez-Bouzas A. An accurate and efficient Bayesian method for automatic segmentation of brain MRI. *IEEE Trans Med Imaging* 2002;21(8):934–45.
- [21] Tian G, Xia Y, Zhang Y, Feng D. Hybrid genetic and variational expectation-maximization algorithm for Gaussian-mixture-model-based brain MR image segmentation. *IEEE Trans Inf Technol Biomed* 2011;15 (3):373–80.
- [22] Prakash M, Kumari RS. Spatial Fuzzy C means and expectation maximization algorithms with bias correction for segmentation of MR brain images. *J Med Syst* 2017;41 (1):1–9.
- [23] Kwon GR, Basukala D, Lee SW, Lee KH, Kang M. Brain image segmentation using a combination of expectation-maximization algorithm and watershed transform. *Int J Imaging Syst Technol* 2016;26(3):225–32.
- [24] Rouainia M, Medjram MS, Doghmane N. Brain MRI segmentation and lesions detection by EM algorithm. *Int J Med Health Sci* 2008;2(12):379–82.
- [25] Bamford J, Sandercock P, Burn M, Warlow JC. Classification and natural history of clinically identifiable subtypes of cerebral infarction. *Lancet* 1991;337:1521–6.
- [26] Gupta M, Chen Y. Theory and use of the EM algorithm. *Found Trends Signal Process* 2010;4(3):223–96.
- [27] Carson C, Belongie S, Greenspan H, Malik J. Blobworld: image segmentation using expectation-maximization and its application to image querying. *IEEE Trans Pattern Anal Mach Intell* 1999;24(8):1026–38.
- [28] Ghamisi P, Couceiro MS, Benediktsson JA, Ferreira N. An efficient method for segmentation of images based on fractional calculus and natural selection. *Expert Syst* 2012;39(16):12407–1.
- [29] Subudhi A, Sahoo S, Biswal P, Sabut S. Segmentation and classification of ischemic stroke using optimized features in brain MRI. *Biomed Eng: Appl Basis Commun* 2018;30 (3):1850011.
- [30] Haralick RM, Shanmugam K, Dinstein I. Textural features for image classification. *IEEE Trans Syst Man Cybern* 1973; SMC-3(6):610–21.
- [31] Breiman L. Random forests. *Mach Learn* 2001;45(1):5–32.
- [32] Quinlan JR. Induction of decision trees. *Mach Learn* 1986;1 (1):81–106.
- [33] Assia C, Yazid C, Said M. Segmentation of brain MRIs by support vector machine: detection and characterization of strokes. *J Mech Med Biol* 2015;15(5):1–23.
- [34] Subudhi AK, Jena SS, Sabut SK. Delineation of the ischemic stroke lesion based on watershed and relative fuzzy connectedness in brain MRI. *Med Biol Eng Comput* 2018;56 (5):795–807.
- [35] Muda AF, Saad NM, Abu-Bakar SR, Muda AS, Abdullah AR. Brain lesion segmentation using fuzzy C-means on diffusion-weighted imaging. *ARPN J Eng Appl Sci* 2015;10 (3):1138–44.
- [36] Griffis JC, Allendorfer JB, Szaflarski JP. Voxel-based Gaussian naive Bayes classification of ischemic stroke lesions in individual T1-weighted MRI scans. *J Neurosci Methods* 2016;257:97–108.
- [37] Mitra J, Bourgeat P, Fripp J, Ghose S, Rose S, Salvado O, Connelly A, Campbell B, Palmer S, Sharma G, Christensen S, Carey L. Lesion segmentation from multimodal MRI using random forest following ischemic stroke. *Neuroimage* 2014;98:324–35.
- [38] Kamal H, Lopez V, Sheth SA. Machine learning in acute ischemic stroke neuroimaging. *Front Neurol* 2018;9:945.
- [39] Raghavendra U, Fujita H, Bhandary SV, Gudigara A, Hong JJ, Tan JH, Acharya UR. Deep convolution neural network for accurate diagnosis of glaucoma using digital fundus images. *Inf Sci* 2018;441:41–9.
- [40] Maier O, Wilms M, Gablentz J, Kramer U, Handels H. Ischemic stroke lesion segmentation in multi-spectral MR images with support vector machine classifiers. *SPIE Medical Imaging Computer-Aided Diagnosis* 2014;9035.